APPLIED AND ENVIRONMENTAL MICROBIOLOGY, June 2006, p. 3814–3825 Vol. 72, No. 6
0099-2240/06/$08.00+0 doi:10.1128/AEM.00119-06

Yersiniabactin Production by *Pseudomonas syringae* and *Escherichia coli*, and Description of a Second Yersiniabactin Locus Evolutionary Group

Alain Bultreys,[1]* Isabelle Gheysen,[1] and Edmond de Hoffmann[2]

Département Biotechnologie, Centre Wallon de Recherches Agronomiques, B-5030 Gembloux,[1] and Laboratoire de Spectrométrie de Masse, Université Catholique de Louvain, B-1348 Louvain-la-Neuve,[2] Belgium

Received 17 January 2006/Accepted 6 March 2006

The siderophore and virulence factor yersiniabactin is produced by *Pseudomonas syringae*. Yersiniabactin was originally detected by high-pressure liquid chromatography (HPLC); commonly used PCR tests proved ineffective. Yersiniabactin production in *P. syringae* correlated with the possession of *irp1* located in a predicted yersiniabactin locus. Three similarly divergent yersiniabactin locus groups were determined: the *Yersinia pestis* group, the *P. syringae* group, and the *Photorhabdus luminescens* group; yersiniabactin locus organization is similar in *P. syringae* and *P. luminescens*. In *P. syringae* pv. tomato DC3000, the locus has a high GC content (63.4% compared with 58.4% for the chromosome and 60.1% and 60.7% for adjacent regions) but it lacks high-pathogenicity-island features, such as the insertion in a tRNA locus, the integrase, and insertion sequence elements. In *P. syringae* pv. tomato DC3000 and pv. phaseolicola 1448A, the locus lies between homologues of Psyr_2284 and Psyr_2285 of *P. syringae* pv. syringae B728a, which lacks the locus. Among tested pseudomonads, a PCR test specific to two yersiniabactin locus groups detected a locus in genospecies 3, 7, and 8 of *P. syringae*, and DNA hybridization within *P. syringae* also detected a locus in the pathovars phaseolicola and glycinea. The PCR and HPLC methods enabled analysis of nonpathogenic *Escherichia coli*. HPLC-proven yersiniabactin-producing *E. coli* lacked modifications found in *irp1* and *irp2* in the human pathogen CFT073, and it is not clear whether CFT073 produces yersiniabactin. The study provides clues about the evolution and dispersion of yersiniabactin genes. It describes methods to detect and study yersiniabactin producers, even where genes have evolved.

Iron is essential for life in nearly all microorganisms. However, it is not readily available because the solubility of ferric ions at neutral pH is very low, and generally iron exists precipitated or chelated to iron-binding proteins in a host and to various compounds in the environment (7, 34, 48, 67). A frequent mechanism used by bacteria to meet their needs for iron is the secretion of low-molecular-mass iron chelating compounds called siderophores. Siderophores are able to solubilize iron and translocate it back to the bacterial cytosol via a specific outer membrane receptor and via transport proteins located in the periplasm and in the inner membrane (7, 67).

Yersiniabactin (YBT) is a bacterial siderophore with a very high stability constant for iron (4×10^{36}) that was characterized in *Yersinia pestis* and *Yersinia enterocolitica* (15, 24, 33, 63). It has been extensively studied because it is a virulence factor widespread among human- and animal-pathogenic enterobacteria. In *Yersinia* spp. (14, 64), the YBT iron uptake system, called the YBT locus (~30 kb), is located in the 36-kb (*Yersinia pseudotuberculosis* and *Y. pestis*) or 43-kb (*Y. enterocolitica*) genomic high-pathogenicity island (HPI). The YBT locus contains one regulatory gene, three genes involved in transport, and the YBT synthesis genes (reviewed in reference 20). The synthesis genes encode Irp4/YbtT of poorly characterized function (32, 54) and, in order of their intervention, the salycilate synthase Irp9/YbtS (62), the salycil-AMP ligase Irp5/YbtE, the peptide synthetase high-molecular-weight protein 2 (HMWP2) (encoded by *irp2*), the polyketide synthase/peptide synthetase HMWP1 (encoded by *irp1*), and the thiazoline reductase Irp3/YbtU. The HPI is found in high-pathogenicity strains of *Y. pestis*, the causal agent of bubonic plague, and of the enteropathogenic species *Y. pseudotuberculosis* and *Y. enterocolitica*. But it is never found in low-pathogenicity or nonpathogenic strains and species. The HPI is mobile due either to its excision mediated by an HPI-encoded P4-like integrase (frequency, $\sim 10^{-4}$) or to an insertion sequence (IS)-mediated deletion of the 102-kb *pgm* locus containing the HPI (frequency, 2×10^{-3}). The HPI is transmissible by horizontal transfer, and it was detected in strains of the human-pathogenic enterobacteria *Escherichia coli*, *Citrobacter* spp., *Klebsiella* spp., *Salmonella enterica*, and *Enterobacter* spp. (4, 55, 58, 71). Modifications were found in these species in the HPI, but the YBT locus was highly conserved. In *E. coli*, the HPI is generally present in human-pathogenic strains of the phylogenetic groups B2 and D, but it is also found in nonpathogenic strains of the phylogenetic groups A and B1 (16, 38). The YBT locus was sequenced in several strains, including three *Y. pestis* strains (21, 60, 80) and *E. coli* CFT073 (84). Recently, genes that are similar to YBT genes have been found in *Corynebacterium diphtheriae* (45), in the insect pathogen *Photorhabdus luminescens* (25), and in two pathovars of the plant pathogen *Pseudomonas syringae* (8, 36).

P. syringae is divided into about 50 pathovars grouped into 9 genospecies; it belongs to the fluorescent pseudomonads, which produce peptide siderophores called pyoverdins (PVDs) (30). Efficient and specific iron-supplying systems appear to be important for fluorescent pseudomonad fitness and competitiveness. Indeed, a diversifying selection occurred in the genes

* Corresponding author. Mailing address: Département Biotechnologie, Centre Wallon de Recherches Agronomiques, Chaussée de Charleroi 234, B-5030 Gembloux, Belgium. Phone: 32 (0) 81 62 73 88. Fax: 32 (0) 81 62 73 99. E-mail: bultreys@cra.wallonie.be.

encoding the *Pseudomonas aeruginosa* PVD peptide chain (79), and numerous siderophore outer membrane receptors are present in the genomes of *P. aeruginosa*, *Pseudomonas putida*, *Pseudomonas fluorescens*, and *P. syringae* (19, 50). *P. syringae*, *Pseudomonas viridiflava*, and *Pseudomonas ficuserectae* produce the same PVD with a stability constant for iron of 10^{25} which is not incorporated by other pseudomonads, except for *Pseudomonas cichorii* (10, 11, 12, 13, 17, 40, 53). This PVD is not essential for growth and virulence of *P. syringae* pv. syringae (18, 47), but it might be useful in competition with other microorganisms under nutritionally poor conditions encountered on the plant surface (10). Since *P. syringae* is an efficient epiphyte and an important plant pathogen (35), a good knowledge of its potential ecological benefits is necessary for developing new methods of population and disease control. Since siderophores play a role in the iron competition-mediated antagonisms between bacteria, the production of a siderophore with a high affinity for iron could be an ecological benefit for a strain.

In this study, methods of producing and detecting YBT (genes) in *P. syringae* and *E. coli* are described. The production of YBT by *P. syringae* is shown to be correlated with the possession of the *irp1* gene, which is located in a recently detected putative YBT locus (8). The *P. syringae* YBT locus is described and compared with similar loci in *Y. pestis* and *P. luminescens*, and it is shown to differ from the usual HPI. The study provides clues about the evolution and dispersion of the YBT genes and describes techniques to detect YBT production (genes) that help in the study of known YBT producers and in finding new ones.

MATERIALS AND METHODS

Bacterial strains and culture conditions. The *Pseudomonas* strains are listed in Table 1. The *E. coli* reference (ECOR) strains (57) were provided by J. R. Johnson, E. Denamur, and B. Picard (Table 2). Precultures were grown at 28°C on medium 2 agar (9) or on nutrient agar. In general, siderophore production was carried out over 3 days in solid-liquid cultures grown unshaken at 20°C in petri dishes containing 10 ml of liquid GASN medium (10) or King's medium B (42) and one block of the corresponding agar medium (10). The culture media were not deferrated, because it has been shown in a previous study (11) that reducing the concentration of iron resulted in the highest activation of siderophore production but reduced total siderophore production because of reduced bacterial growth. The most important total siderophore production was observed when 5 μM Fe(III)-EDTA was added to a Fe-depleted culture medium, when bacteria were slightly repressed in siderophore production but grew abundantly. More importantly, siderophore repression was observed when 10 or 20 μM Fe(III)-EDTA was added to the Fe-depleted culture medium. In this study, procedures to obtain high siderophore production using standard medium constituents were selected. Important siderophore production was observed in solid/liquid GASN and King's B media using the following: osmosed water; Bacto agar and Bacto peptone (Becton Dickinson); L-asparagine, 99% thin-layer chromatography (Sigma); D(+)-glucose anhydrous for biochemistry and KH_2PO_4 and Na_2HPO_4 for analysis (Merck); glycerol bidistilled, 99.5% (wt/vol), K_2HPO_4, and $MgSO_4 \cdot 7H_2O$ for analysis (Prolabo).

Production and HPLC detection of YBT. The high-pressure liquid chromatography (HPLC) method of analyzing Fe(III)-chelated PVD (Fe-PVD) (12) was used to detect Fe(III)-chelated YBT (Fe-YBT) in the culture medium of *Pseudomonas* strains, but the chromatograms were also analyzed at 305 nm because Fe-YBT absorbs more at 305 nm than at 403 nm, which was the wavelength used for Fe-PVD. The HPLC program 2 (12) used was as follows: (A, 17 mM NaOH-acetic acid buffer, pH 5.3; B, acetonitrile, 0.9 ml/min): 100% A, 8 min; from 100% A to 98% A, 2 min; 98% A, 10 min; from 98% A to 95% A, 5 min; from 95% A to 30% A, 15 min; 30% A, 5 min. Before the injection at pH 5.0 to 5.3 in a Nucleosil C_{18} column, the liquid medium from one solid/liquid culture was supplemented with $FeCl_3$, centrifuged, and filtrated; HPLC peaks were identified by their retention times and spectra, with reference to a control in the sample set.

E. coli ECOR 10 (D) and ECOR 20 (D) were grown at 37°C for 4 days in solid-liquid cultures in parafilm-sealed petri dishes. The media tested were as follows: King's medium B, T-medium (77), SN (74), GASN, and single-amino-acid-based media (not shown). *E. coli* strains were then grown in King's medium B for 2 or 4 days, as above, or in 25-ml-containing 100-ml shaken (220 rpm) Erlenmeyer flasks. The pH was set near 7.0 before the addition of $FeCl_3$. YBT production was detected as described above or by using the HPLC program 3 (A, 17 mM NaOH-acetic acid buffer, pH 5.3; B, acetonitrile; 0.9 ml/min): from 95% A to 30% A, 15 min; and 30% A, 5 min.

Purification and characterization of YBT. The recommended procedures for purifying Fe-PVDs and PVDs using a C_{18} column (10, 13) were followed, but the water-methanol fractions were excluded and YBT or Fe-YBT was collected in methanol. Cation-exchange chromatography was carried out for Fe-YBT with a type CM C25 Sephadex column eluted with a 30 mM NaOH-formic acid buffer (pH 4.2). Desalting was carried out in a C_{18} column. Purity was assessed using HPLC. A model Lambda 5 UV/VIS spectrophotometer (Perkin-Elmer) was used for spectrophotometry. YBT was analyzed in water-methanol (40:60, vol/vol); Fe-YBT was analyzed in water and in a 25 mM NaOH-phosphoric acid buffer (pH 7.0). Spectra were also obtained from the photodiode array detector in HPLC analyses. Electrospray-ionization-mass spectrometry (ESI-MS), tandem mass (MS/MS) and MS/MS/MS analyses were obtained using an Ion Trap Finnigan MAT LCQ mass spectrometer in the direct infusion mode.

PCR detection of YBT genes. The cells were grown shaken (200 rpm) overnight in 4 ml of nutrient broth at 28°C. The lysed cells were prepared as previously described (9), but without the passages from −20°C to 70°C. The published primers used were (*irp1*) irp1up and irp1lp (41) and (*fyuA*) FyuA f′ and FyuA r (37). The PCR conditions were as follows: 5×10^5 lysed cells; 30 pmol of each primer; 2 U *Taq* DNA polymerase used with its buffer (Pharmacia); and a concentration of 200 μM of each deoxynucleoside triphosphate (Roche). The programs (iCycler; Bio-Rad) were as follows: an initial denaturation at 94°C for 5 min; 30 cycles at 94°C for 1 min, 58°C (*fyuA*) or 59°C (*irp1*) for 1 min, and 72°C for 1 min; and a final elongation at 72°C for 8 min.

In order to develop a general PCR detection test of *irp1*, *irp1* of *P. syringae* pv. tomato DC3000 and *Y. enterocolitica* WA-C were aligned to find short conserved sequences. Checks were carried out to ensure that these sequences were conserved in known YBT producers and not found in genes encoding proteins from other species that were found with BLASTP to be similar to the *irp1* product HMWP1. The proteins checked in this way were HMWP1 from *P. syringae* pv. tomato (NP_792409), *Y. enterocolitica* (CAA73127), and *Y. pestis* (NP_405471); the c_2427, c_2428, c_2429 and c_2460 proteins from *E. coli* (NP_754319, NP_754320, NP_754321, and NP_754352); NrpS from *Proteus mirabilis* (AAD10390); Plu2321 from *P. luminescens* (NP_929573); COG1020 from *Desulfovibrio desulfuricans* (ZP_00130212) and *P. syringae* pv. syringae (ZP_00124542); COG3321 from *Nostoc punctiforme* (ZP_00111186) and *Trichodesmium erythraeum* (ZP_00074380); MtaD from *Stigmatella aurantiaca* (AAF19812); EPOS B from *Polyangium cellulosum* (AAF26920); and PpsE from *Mycobacterium tuberculosis* (NP_217451). The selected sequences were evaluated as primers in PCR tests (not shown). The primers selected for screenings were PSYE2 (5′-GGCACCTGGAACAGG-3′) and PSYE2R (5′-GCCAGATCGTC CATCAT-3′) (product, 943 bp in *P. syringae* and 925 bp in *E. coli*); 25 pmol of each primer and 1 U *Taq* DNA polymerase were used, and the program was as follows: an initial denaturation at 94°C for 4 min; 37 cycles at 94°C for 1 min, 64°C for 1 min, and 72°C for 1 min, and then a final elongation at 72°C for 6 min. The *E. coli* 925-bp and *P. syringae* 943-bp expected PCR products were 64.2% identical (Align).

To take account of a modification in *P. syringae* pv. phaseolicola 1448A at the last but one base in the 3′-end region of the primer PSYE2, the primer PSYE4 (5′-TGGCACCTGGAACA-3′) was tested with the reverse primers PSYE4R (5′-GCCAGATCGTCCATC-3′) (product, 896 bp; annealing temperature, 57°C) and PSYE5R (5′-GCCAGATCGTCCATC-3′) (product, 944 bp; annealing temperature, 57°C); nevertheless, there was still one base difference in the middle of the region corresponding to PSYE4 in *P. syringae* pv. phaseolicola 1448A.

DNA hybridization. The 943-bp PCR product obtained with *P. syringae* pv. tomato LMG 5093 using the primers PSYE2 and PSYE2R was purified using a QIAquick PCR purification kit (QIAGEN) and used to construct an [α-^{32}P]dCTP-marked radioactive probe using an RPN 1604 kit (Amersham). Dot blots were performed using about 5 μg of DNA per strain, purified as previously described (9), positively charged nylon membranes, and standard protocols (3). The strains analyzed were as follows: PCR-positive control strains of *P. syringae* from different genospecies, all the PCR-negative strains of *P. syringae* and of the genet-

TABLE 1. Characteristics of *Pseudomonas* strains

Strain[a]	Origin	Country	Strain genospecies[b] (pathotype)	Yersiniabactin analysis[c]				
				HPLC result and MS-measured ion[d]	PCR test result for the following gene and primers:			Dot blot result[e]
					fyuA; FyuA f′, FyuA r	*irp1*; irp1up, irp1lp	*irp1*; PSYE2, PSYE2R	
P. syringae pv. aceris LMG 2106^T	Unknown	Unknown	1	−	NT	NT	−	−
P. syringae pv. aptata LMG 5059^T	Sugar beet	United States	1	−	NT	NT	−	−
P. syringae pv. atrofaciens LMG 5095^T	Wheat	New Zealand	1	−	NT	NT	−	−
P. syringae pv. dysoxyli LMG 5062^T	*Dysoxylum spectabile*	New Zealand	1	−	NT	NT	−	−
P. syringae pv. japonica LMG 5068^T	Barley	Japan	1	−	NT	NT	−	−
P. syringae pv. lapsa LMG 2206^T	*Zea* sp.	Unknown	1	−	NT	NT	−	−
P. syringae pv. panici LMG 2367^T	Unknown	Unknown	1	−	NT	NT	−	−
P. syringae pv. papulans LMG 5076^T	Apple	Canada	1	−	NT	NT	−	−
P. syringae pv. pisi LMG 5079^T	Pea	New Zealand	1	−	NT	NT	−	−
P. syringae pv. syringae LMG 1247^T	Lilac	England	1	−	NT	NT	−	−
P. syringae pv. ciccaronei LMG 5541^T	*Ceratonia siliqua*	Italy	2	−	NT	NT	−	−
P. syringae pv. eriobotryae LMG 2184^T	*Eriobotrya japonica*	United States	2	−	NT	NT	−	−
P. syringae pv. glycinea LMG 5515	Soybean	Canada	ND (2)	−	NT	NT	−	+
P. syringae pv. mellea LMG 5072^T	Tobacco	Japan	2	−	NT	NT	−	−
P. syringae pv. mori LMG 5074^T	White mulberry	Hungary	2	−	NT	NT	−	−
P. syringae pv. myricae LMG 5668^T	*Myrica rubra*	Japan	2	−	NT	NT	−	−
P. syringae pv. phaseolicola LMG 2245^T	Bean	Canada	2	−	−	−	−	+
P. syringae pv. savastanoi LMG 2209^T	Common olive	Yugoslavia	2	−	NT	NT	−	−
P. syringae pv. sesami LMG 2289^T	Sesame	Yugoslavia	2	−	NT	NT	−-	−
P. syringae pv. tabaci LMG 5393^T	Tobacco	Hungary	2	−	NT	NT	−	−
P. syringae pv. ulmi LMG 2349^T	Elm	Yugoslavia	2	−	NT	NT	−	−
P. syringae pv. antirrhini LMG 5057^T	Snapdragon	England	3	−	−	−	+	NT
P. syringae pv. apii LMG 2132^T	Celery	United States	3	+, 535	−	−	+	NT
P. syringae pv. berberidis LMG 2147	Barberry	New Zealand	ND (3)	+, 535	−	−	+	NT
P. syringae pv. delphinii LMG 5381^T	Larkspur	New Zealand	3	+, 535	−	−	+	+
P. syringae pv. lachrymans LMG 5070^T	Cucumber	United States	3	+, 535	−	−	+	+
P. syringae pv. maculicola LMG 5295	Radish	United States	ND (3)	−	NT	NT	−	−
P. syringae pv. passiflorae LMG 5185^T	*Passiflora edulis*	New Zealand	3	−	−	−	+	NT
P. syringae pv. persicae LMG 5184^T	Peach	France	3	+, 535	−	−	+	NT
P. syringae pv. ribicola LMG 2276^T	Currant	Unknown	3	−	NT	NT	−	−
P. syringae pv. tomato strains								
LMG 5093^T	Tomato	England	3	+, 535	−	−	+	+
LMG 5155	Tomato	United States	ND	+, 535	−	−	+	NT
LMG 5507	Tomato	Canada	ND	+, 535	−	−	+	NT
LMG 5508	Tomato	Switzerland	ND	+	−	−	+	NT
LMG 5509	Tomato	New Zealand	ND	+	−	−	+	NT
P. syringae pv. viburni LMG 2351^T	Arrowwood	United States	3	−	−	−	+	NT
P. syringae pv. coronafaciens strains								
LMG 5060^T	Oat	England	4	−	NT	NT	−	NT
LMG 2330	Unknown	Unknown	ND	−	NT	NT	−	−
P. syringae pv. garcae LMG 5064^T	Coffee	Brazil	4	−	NT	NT	−	−
P. syringae pv. oryzae LMG 10912^T	Rice	Japan	4	−	NT	NT	−	−
P. syringae pv. primulae LMG 2252^T	Primrose	United States	6	−	NT	NT	−	−
P. syringae pv. helianthi LMG 5067^T	Mirasol	Mexico	7	+, 535	−	−	+	+
P. syringae pv. tagetis LMG 5090^T	Marigold	Zimbabwe	7	+, 535	−	−	+	+
P. syringae pv. theae LMG 5092^T	Tea	Japan	8	+, 535	−	−	+	+
P. syringae pv. morsprunorum race 1 LMG 2222	Sweet cherry	England	ND (2, 3)	−	NT	NT	−	−
P. syringae pv. morsprunorum race 2 strains			ND					
CFBP 3798	*Prunus* sp.	England		−	−	−	+	NT
CFBP 3799	Sour cherry	England		+	−	−	+	NT
CFBP 3800	Sour cherry	England		+	−	−	+	NT
Pm2C69	Sour cherry	Belgium		+	−	−	+	NT
Pm2C76	Sour cherry	Belgium		−	−	−	+	NT
Pm2C86	Sour cherry	Belgium		−	−	−	+	NT
Pm2C92	Sour cherry	Belgium		−	−	−	+	NT
P. viridiflava LMG 2352^T	Bean	Switzerland	6	−	NT	NT	−	−
P. meliae LMG 2220^T	*Melia azedarach*	Japan	2	−	NT	NT	−	−

Continued on following page

TABLE 1—*Continued*

Strain[a]	Origin	Country	Strain genospecies[b] (pathotype)	Yersiniabactin analysis[c]				
				HPLC result and MS-measured ion[d]	PCR test result for the following gene and primers:			Dot blot result[e]
					fyuA; FyuA f′, FyuA r	*irp1*; irp1up, irp1lp	*irp1*; PSYE2, PSYE2R	
P. ficuserectae LMG 5694^T	*Ficuserecta*	Japan	2	−	NT	NT	−	−
P. cichorii LMG 2162^T	Endive	Germany		−	−	−	−	NT
P. asplenii LMG 2137	Fern	Unknown		−	NT	NT	−	NT
P. fuscovaginae LMG 2158^T	Rice	Japan		−	NT	NT	−	NT
P. agarici LMG 2112^T	*Agaricus bisporus*	New Zealand		−	NT	NT	−	NT
P. marginalis LMG 14572	Dahlia	Unknown		−	NT	NT	−	NT
P. marginalis pv. *marginalis* LMG 5177	Bean	Unknown		−	NT	NT	−	NT
P. fluorescens LMG 1794^T	Water	England		−	−	−	−	NT
P. chlororaphis LMG 5004^T	Contaminated plate	Unknown		−	NT	NT	−	NT
P. putida LMG 2257^T	Soil	United States		−	−	NT	−	NT

[a] LMG, Laboratorium voor Microbiologie van Gent; CFBP, Collection Française de Bactéries Phytopathogènes; T, type or pathotype.
[b] Data from reference 30 obtained by DNA-DNA hybridization; ND, not determined; the number in parentheses is the genomic species of the pathotype strain when it was not used in this study.
[c] Data from this study; NT, not tested.
[d] + and −, results of the HPLC analyses; the number is the nominal ion (*m*/*z*) measured in ESI-MS positive-ion analyses after Fe-YBT purification, when analyzed.
[e] Dot blot results using the most stringent washing conditions.

ically closely related species, and PCR-positive as well as PCR-negative *E. coli* strains. The most stringent final washing conditions were as follows: 0.1× SSC (1× SSC is 0.15 M NaCl plus 0.015 M sodium citrate [3])–0.1% sodium dodecyl sulfate (SDS); 75°C. Intermediate final washing conditions were as follows: 0.1× SSC–0.1% SDS; 55.5°C. The lowest stringent final washing conditions were as follows: 0.2× SSC–0.1% SDS; 49°C. The membranes were read using a model Molecular Imager^R FX and the program Quantity one^R (Bio-Rad).

Comparisons of the YBT loci and map constructions. The BLAST programs (1, 81), Conserved Domain Search, and annotated sequences were used or obtained from the National Center for Biotechnology Information. The sequences used to compare the YBT loci were as follows: *P. syringae* pv. tomato DC3000 AE016864, AE016865, and AE016866; *P. syringae* pv. syringae B728a NC_007005; *P. syringae* pv. phaseolicola 1448A NC_005773; *Y. pestis* 91001 AE017133; *P. luminescens* TTO1 BX571866; *E. coli* CFT073 AE016762; *Y. enterocolitica* L18881, Z35486 (8081), and Z29675 (WA-C); *Y. pseudotuberculosis* IA Z35107; *C. diphtheriae* NCTC13129 NC_002935; and *P. aeruginosa* PAO1 X82644. The GC content, identities, and similarities were obtained using Freqsq, Align, Ssearch (56, 78; http://www.infobiogen.fr), BLASTP, BLASTN, and BLAST 2 Sequences. The maps were constructed using Vector NTI (InforMax, Inc.) or PowerPoint.

Search for mutations in *irp1 and irp2* in *E. coli*. In order to determine whether the modifications in *irp1*, *irp2*, and *irp5* found in *E. coli* CFT073 give functional proteins in *E. coli*, a search for the modifications in *irp1* and *irp2* was undertaken with YBT-producing ECOR strains. The *irp1* segments modified in *E. coli* CFT073 were sequenced in six ECOR strains. Primer3 (http://www.be.embnet.org) was used to select the primers irp1122 (5′-GCGATTGTCGCGTTTGAAATC-3′) for c_2427 and irp1121R (5′-GCCAGTAATCCGCCTGGTTG-3′) for c_2428 (product, 540 bp in CFT073), and irp1232 (5′-AGTCATGGCTACGCG

TABLE 2. Characteristics of *E. coli* strains

E. coli strain[a]	Origin	Country	Phylogenetic group[b]	Yersiniabactin analysis[c]				
				HPLC result	PCR test result for the following gene and primers:			Dot blot result[e]
					fyuA; FyuA f′, FyuA r	*irp1*; irp1up, irp1lp	*irp1*; PSYE2, PSYE2R	
ECOR 1	Human	United States	A	−	−	−	−	− (P)
ECOR 3	Dog	United States	A	−	−	−	−	− (P)
ECOR 4 (P)	Human	United States		+	+	+	+	+
ECOR 4 (D) (J)	Human	United States	A	−	−	−	−	NT
ECOR 10[d]	Human	United States	A	+	+	+	+	+ (P)
ECOR 13[d]	Human	Sweden	A	−	−	−	−	− (P)
ECOR 18[d]	Celebes ape	United States	A	−	−	−	−	− (P)
ECOR 20[d]	Steer	India	A	−	−	−	−	− (P)
ECOR 22	Steer	India	A	−	−	−	−	− (P)
ECOR 67	Goat	Indonesia	B1	−	−	−	−	− (J)
ECOR 69 (P) (D)	Celebes ape	United States		+	+	+	+	+ (P)
ECOR 69 (J)[d]	Celebes ape	United States	B1	−	−	−	−	NT

[a] (P), obtained from B. Picard (University of Brest, France); (D), obtained from E. Denamur (Faculty of Medicine Xavier Bichat, Paris, France); (J), obtained from J. R. Johnson (University of Minnesota, Minneapolis); no notation, identical results for three origins.
[b] Information from reference 38.
[c] Data from this study.
[d] Strain previously noted as possessing *fyuA* (38). However, recent reassessments using the same method as used previously confirmed the result presented here (J. R. Johnson, personal communication).
[e] Dot blot results using the intermediate and lowest stringent washing conditions; NT, not tested; since only one origin was tested for each reference strain, the origin of the tested strain is specified with the result.

ACGTG-3′) in c_2428 and irp1232R (5′-CATCACCGCCTGTTCCAGGT-3′) in c_2429 (product, 510 bp in CFT073). The PCR conditions were as for PSYE2/PSYE2R, but 1 ng of purified DNA, 30 pmol of each primer, and 2 U *Taq* DNA polymerase were used; the annealing temperature was 69°C. The products were purified using a QIAquick PCR purification kit (QIAGEN). Sequencing was carried out with 500 ng of DNA and IRD800-labeled primers (Biolegio) by using the DYEnamic Direct cycle sequencing kit (Amersham Biosciences). The products were loaded into a model 4200 IR^2 DNA sequencer (LI-COR) and analyzed with e-Seq (LI-COR). The forward primers used to detect the CFT073 IS*1541A*-like due insertion in *irp2* (i.e., caused by an IS element similar to an IS*1541A* element) were irp2121 (5′-CCTTACCGCTGACGGCTA-3′) and irp2122 (5′-ACCCCTGAAGCGGAAAAC-3′) for c_2424. The reverse primers were irp2121R (5′-CGCCTTGCTGGAAGAAGT-3′) and irp2122R (5′-CGCTTCATAACCTGCCTGA-3′) for c_2426. The expected product was 900 (2121/2121R), 959 (2121/2122R), 843 (2122/2121R), or 903 bp (2122/2122R) in the presence of the insertion and 189, 248, 132, or 192 bp in its absence. The PCR conditions were as for PSYE2/PSYE2R, but the annealing temperature was 61°C.

RESULTS

Production and HPLC detection of YBT. Fe-YBT was detected during the Fe-PVD purification of *P. syringae* pv. tomato LMG 5093, because a reddish-orange compound remained adsorbed in the C_{18} column after Fe-PVD elution. In the absence of iron, the compound was colorless in the column and in methanol, but it readily turned reddish-orange following the addition of $FeCl_3$. While YBT was characterized, the Fe-YBT peak was detected using the HPLC method for analyzing Fe-PVD production in fluorescent pseudomonads (Fig. 1A). It was then detected, using HPLC, in *P. syringae* genospecies 3, 7, and 8 and pathovar morsprunorum race 2 (Table 1). GASN medium was generally used, but strains of pathovars apii and persicae produced YBT only in King's medium B. PVD-nonproducers, such as *P. syringae* pv. persicae LMG 5184 and *P. syringae* pv. tomato LMG 5155, produced YBT, but others did not (not shown).

With regard to *E. coli*, the 10 ECOR strains were initially chosen because they belong to the nonpathogenic phylogenetic groups A and B1 and because 5 of them had been previously found to possess the YBT receptor gene *fyuA* (38; Table 2). Single-amino-acid-based media proved to be inefficient for inducing YBT production by *E. coli*. Growing *E. coli* at 37°C for 48 h in King's medium B was the best way to produce YBT (not shown). In one experiment, the Fe-YBT HPLC peak area at 403 nm was 2.4, 7.6, 7.2, 12.4, 13.4, or 7.0 times higher, depending on the strain, using the solid-liquid technique with petri dishes rather than shaken Erlenmeyer flasks (Fig. 1B and 2). However, the HPLC results did not always accord with published data, and the results with ECOR 4 and ECOR 69 obtained from three origins did not always agree with each other (Table 2).

Purification of YBT. Due to the YBT hydrophobicity, a one-step purification of YBT from the very simple GASN medium enabled us to characterize it. Ion-exchange chromatography further improved Fe-YBT purity and facilitated its purification from King's medium B. Purification was carried out for YBT of *P. syringae* pv. tomato LMG 5093 and for Fe-YBT of the strains for which the ion 535 is specified in Table 1.

Chemical characterization of YBT. The spectrophotometric analyses accorded with data for YBT (15, 24, 33, 63): the free molecule (M) showed absorbance maxima near 207, 251, and 310 nm in water-methanol; and the Fe molecule showed absorbance maxima near 227, 255, 305, and 386 nm in water, in phosphate buffer (pH 7.0), and under the HPLC conditions. FeM from *P. syringae* and Fe-YBT from *E. coli* showed similar retention times and absorbance maxima (Fig. 1A and B) in HPLC analyses. MS analyses indicated that M and FeM had the same molecular masses and split at the same places to produce the same fragments as YBT. Indeed, ESI-MS of M produced an $[M+H]^+$ ion of *m*/*z* 482.2, as related for YBT (24). Then, in their ESI-MS characterization of Fe-YBT, Drechsel et al. (24) observed the monomer (*m*/*z* 535), the dimer, and the trimer of the iron complex, as well as a dominant iron ion of an uncharged fragment of 295, which actually corresponds to an ion $[295\text{-}2H+Fe]^+$ of *m*/*z* 349 resulting from the loss of a described uncharged 186 fragment from the monomer. As expected for YBT, in the present study (Fig. 1C), ESI-MS of FeM carried out using an ion trap mass spectrometer produced the ions $[FeM+H]^+$ of *m*/*z* 535.1 and $[FeM+H\text{-}186]^+$ of *m*/*z* 349.1, as well as the other characteristic ions (24, 63) of *m*/*z* 557.2 (monomer Na adduct), 1,068.8 (dimer), 1,090.8 (dimer Na adduct), and 1,602.7 (trimer). In addition, MS/MS confirmed that 883.0 (Fig. 1C) is the one-charge combination of 349.1 and 535.1, and MS/MS/MS analyses gave an ion of *m*/*z* 192.5 corresponding to the positive ion of an uncharged fragment of 191 also described by Drechsel et al. (24). Finally, MS/MS of 535.1 produced the described ion of *m*/*z* 489.0 (63) and other ions also found in the other analyzed pathovars (Table 1).

General PCR detection of *irp1* and DNA hybridization. Although efficient with *E. coli* (Table 2), the primers irp1up/irp1lp and FyuA f′/FyuA r were inefficient for all the YBT-producing *P. syringae* strains (Table 1).

Only four conserved 17-bp sequences were found between *irp1* of *Y. enterocolitica* WA-C and *irp1* of *P. syringae* pv. tomato DC3000 located in a putative YBT locus in the genome of this strain (8), and no sequence was also conserved in a similar locus in *P. luminescens* TTO1 (25). The PSYE2/PSYE2R primer pair was selected. PSYE2 is conserved in *Y. pestis* and *E. coli*, but there is one base substitution in PSYE2R in both species, whereas there are six and nine base substitutions in *P. luminescens*.

In *P. syringae*, the detection of YBT by HPLC correlated with the PCR detection of the *irp1* gene located in the putative YBT locus of *P. syringae* DC3000 and 1448A, which accords with the putative function assigned to these loci (Table 1) (8, 36). Also, the concordant results obtained with YBT-positive strains using two *irp1*-based PCR tests were indicative of the similarity in the *irp1* gene sequence in the different *P. syringae* pathovars. However, seven strains in pathovars antirrhini, passiflorae, viburni, and morsprunorum race 2 were negative using HPLC but positive using PCR. Among the 25 strains tested from genospecies 3, 7, and 8 and pathovar morsprunorum race 2, only *P. syringae* pv. maculicola LMG 5295 and *P. syringae* pv. ribicola LMG 2276 were negative using PCR. All the strains from other genospecies and from other *Pseudomonas* species were negative using PCR. A good conservation of *irp1* was observed in the pathovars tomato and morsprunorum race 2.

For *E. coli*, the PCR results confirmed all the HPLC results (Table 2).

Dot blot using the most stringent washing conditions con-

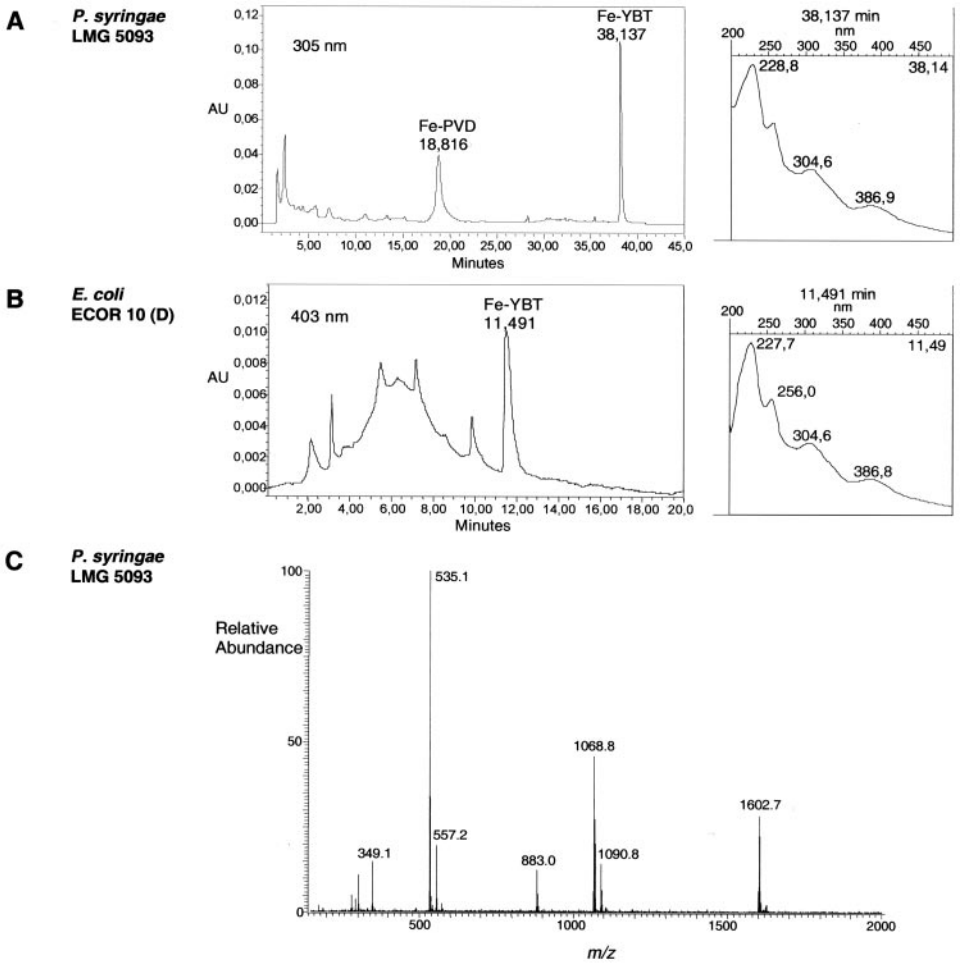

FIG. 1. Detection (A) in GASN medium with the HPLC program 2 of Fe-PVD and Fe-YBT produced by *P. syringae* pv. tomato LMG 5093 and (B) in King's medium B with the HPLC program 3 of Fe-YBT produced by *E. coli* ECOR 10. For each strain, an HPLC analysis (on the left) and the spectral characteristics of Fe-YBT analyzed in line (on the right) are shown. Both HPLC programs can be used for each species. In King's medium B (B), Fe-YBT is more easily detected at 403 nm because medium components (visible between 2 and 10 min) absorb more at 305 nm. (C) ESI-MS positive-ion analysis of Fe-YBT of *P. syringae* pv. tomato LMG 5093.

firmed all the PCR results for *P. syringae* and the genetically closely related species, except that an *irp1* homologue was detected in *P. syringae* pv. phaseolicola LMG 2245 and *P. syringae* pv. glycinea LMG 5515 (Table 1); the identity of *P. syringae* pv. phaseolicola 1448A *irp1* with the probe is 87.5%. The PCR-positive *E. coli* ECOR 4 (P), ECOR 10 (P), and ECOR 69 (P) gave negative results in these conditions, as expected given the low sequence identity of *E. coli irp1* with the probe (64.2%). The use of the intermediate or the lowest stringent washing conditions confirmed the results for the pathovars phaseolicola and glycinea, and it enabled the very probable detection of the *irp1* homologues in *E. coli* ECOR 4 (P), ECOR 10 (P), and ECOR 69 (P) (Table 2). But only clearly weaker signals, or no signals, were observed for all the other PCR-negative *Pseudomonas* and *E. coli* strains analyzed, which indicated an identity clearly inferior to 64% and confirmed the very probable absence of a YBT locus in all these strains.

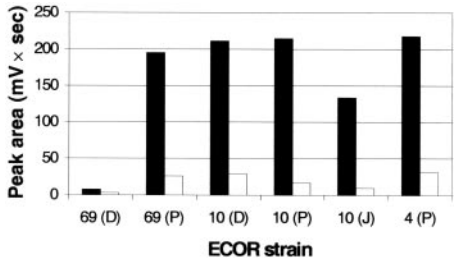

FIG. 2. YBT production in King's medium B by the *E. coli* strains ECOR 69, ECOR 10, and ECOR 4 received from different origins: (P), received from B. Picard; (D), received from E. Denamur; and (J), received from J. R. Johnson (Table 2). The strains were grown at 37°C for 2 days in either one still petri dish with one agar block (black bars) or one shaken Erlenmeyer flask (white bars). YBT production was assessed by the Fe-YBT HPLC peak area at 403 nm.

The new primers PSYE4, PSYE4R, and PSYE5R take account of the *irp1* sequence in *P. syringae* pv. phaseolicola 1448A, and they were workable with both YBT-positive *P. syringae* and *E. coli* strains. But the attempts to find general PCR conditions that would also be workable with *P. syringae* pv. phaseolicola LMG 2245 and *P. syringae* pv. glycinea LMG

TABLE 3. Similarity search between *P. syringae* and *Y. pestis* or *P. luminescens* proteins

Protein[a] (aa[b]) of *P. syringae* DC3000	Proposed new name	Homologous protein[a] (aa[b]) of *Y. pestis* 91001	% Identity–% similarity (amino acid overlap)[c]	Homologous protein[a] (aa[b]) of *P. luminescens* TTO1	% Identity–% similarity (amino acid overlap)[c]
PchA (469)		YbtS (434)	27.6–52.9 (420)	Plu2324 (977)	27.3–53.4 (457)
Irp5 (522)		YbtE (525)	57.5–81.0 (515)	Plu2324 (977)	56.4–79.2 (514)
Irp4 (271)		YbtT (267)	50.8–71.0 (238)	Plu2323 (258)	52.8–74.4 (250)
Irp3 (360)		YbtU (386)	49.9–72.9 (343)	Plu2322 (365)	46.0–72.3 (361)
HMWP1 (3,173)		HMWP1 (3,163)	52.6–76.0 (3,187)	Plu2321 (3,908)	41.3–62.8 (3,211)
PSPTO2601 (408)	Irp8	YbtX (467)	29.2–60.1 (404)	Plu2317 (414)	30.7–62.1 (378)
PSPTO2602 (2,057)	HMWP2	HMWP2 (2,041)	52.3–74.2 (2,045)	Plu2320 (2,049)	51.2–74.6 (2,053)
PSPTO2603 (581)	Irp7	YbtQ (600)	33.1–65.8 (564)	Plu2319 (600)	34.2–65.6 (582)
PSPTO2604 (593)	Irp6	YbtP (600)	37.9–66.6 (578)	Plu2318 (575)	38.8–68.0 (557)
PSPTO2605 (685)	FyuA	FyuA (673)	32.2–61.7 (652)	Plu2316 (668)	35.3–66.4 (651)
PSPTO2606 (312)	YbtA	YbtA (319)	30.8–60.9 (169)	Plu2315 (323)	30.4–59.5 (289)

[a] Protein names accord with the annotated genomes.
[b] No. of amino acids.
[c] Data obtained using Ssearch.

5515 remained surprisingly unsuccessful, which probably reflects additional sequence variations in both strains.

Sequence comparisons between YBT locus genes. Comparisons were carried out between confirmed or putative YBT genes and proteins of different species, and three groups were identified. This is illustrated by *irp2* (Align): *irp2* from *Y. pestis* 91001 had 98% identity with its homologue in *Y. enterocolitica* 8081, 98.5% with that in *E. coli* CFT073 (without an IS*1541A*-like due 711-bp insertion), but only 59.9% with that in *P. syringae* DC3000 and 55.7% with that in *P. luminescens* TTO1, whereas *irp2* homologues of the latter two species showed only 55.9% identity.

Functionally comparable predicable proteins were found in the YBT loci of *Y. pestis*, *P. syringae*, and *P. luminescens*. Similarities were found between these proteins, and names to use when referring to the *Y. enterocolitica* nomenclature are proposed for *P. syringae* because it produces YBT (Table 3). Both *P. syringae* and *Y. pestis* proteins differed about equally from those of the other species, which confirmed the existence of three YBT locus evolutionary groups. HMWP1 of *P. syringae* and that of *Y. pestis* were about 740 amino acids (aa) shorter than Plu2321 of *P. luminescens* (Table 3), and the similarity in the overlap was lower when Plu2321 was compared with HMWP1 of *P. syringae* (62.8%) or *Y. pestis* (65.5% similarity in a 2,923-aa overlap) than when HMWP1 of *P. syringae* and *Y. pestis* were compared to each other (76.0%). This was not observed for HMWP2 (Table 3).

HMWPI and HMWP2 of *P. syringae* DC3000 had a relatively

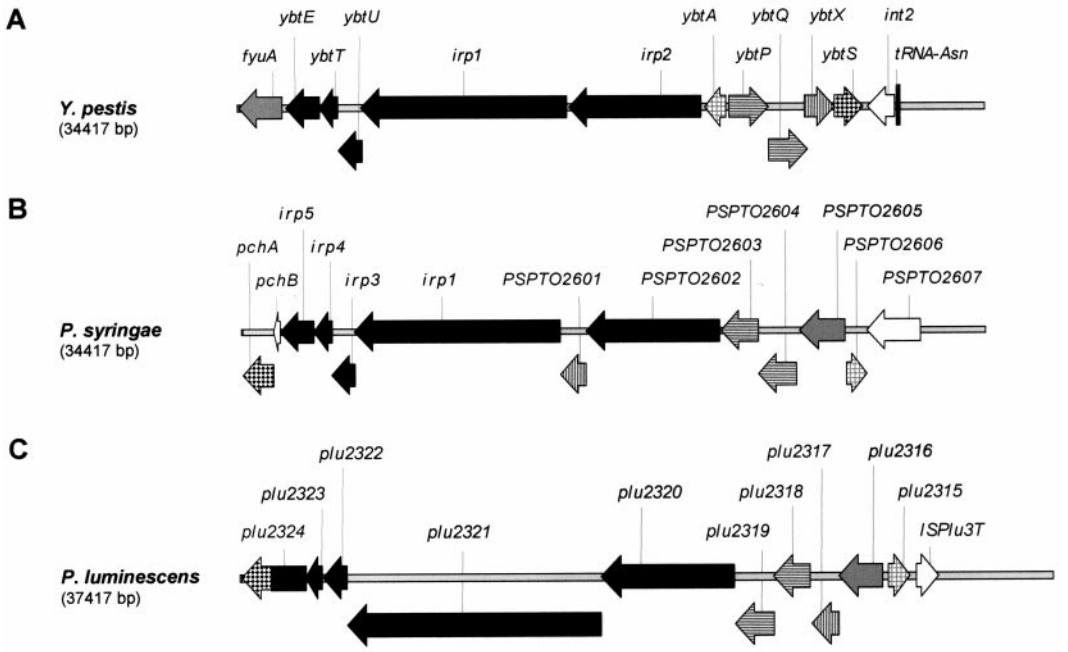

FIG. 3. Map of the YBT locus in (A) *Y. pestis* 91001, (B) *P. syringae* DC3000, and (C) *P. luminescens* TTO1, according to annotated genomes. The genes are designed according to the encoded protein functions: black, biosynthetic enzymes, apart from *ybtS* homologues, represented by a dark squaring; gray, membrane receptors; horizontal lines, transport proteins; light squaring, regulatory proteins; and vertical lines, proteins of unknown function. The white-coded genes have no homologues in the other species.

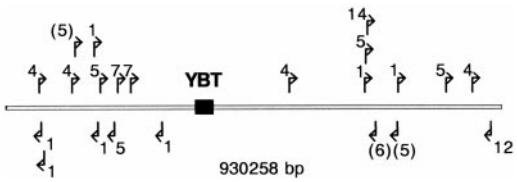

FIG. 4. Map and orientation of IS elements around the YBT locus (black box) of *P. syringae* DC3000 according to the annotated genome: 1, IS*Pssy*; 4, IS*Psy4*; 5, IS*Psy5*; 6, IS*Psy6*; 7, IS*Psy7*; 12, IS*Psy12*; 14, IS*Psy14*. The parentheses indicate disrupted IS elements.

weak similarity of 53.5% (2,413-aa overlap) and 51.0% (2,061-aa overlap) with DIP2160 and DIP2161, respectively, from *C. diphtheriae* NCTC13129, whose coding genes *sidB* and *sidA* are similar to *Y. pestis irp1* and *irp2* (45).

Gene organization. The YBT locus organization of *P. syringae* is closer to that of *P. luminescens* than that of *Y. pestis* (Fig. 3). Two differences are the position of *irp8* of *P. syringae* (PSPTO2601) between *irp1* and *irp2* (PSPTO2602) and the fusion of the *irp5* and *pchA* homologues in *P. luminescens* (plu2324). In contrast with *Y. pestis*, the latter two genes are also close together in *P. syringae* but separated by *pchB*. It is worth noting that in the *P. syringae* YBT locus there is no insertion in a tRNA locus, no integrase, and no IS element in its proximity (Fig. 4), whereas an integration in an *asn* tRNA locus, the integrase-coding *int2*, and IS elements on both sides of the represented genes are present in *Y. pestis*, and IS*Plu3T* is present in *P. luminescens* (Fig. 3). In *P. syringae*, PSPTO2607 encodes an additional putative siderophore receptor on the right border of the cluster (Fig. 3B). The GC content of the YBT locus of *P. syringae* DC3000 is 63.4%, which is higher than the mean value of 58.4% for the chromosome (8).

In *Y. pestis*, YbtS converts chorismate to salicylate in YBT synthesis (31, 62), but PchA and PchB are necessary for this conversion in *P. aeruginosa* in pyochelin synthesis (28, 29, 75). PchA of *P. syringae* DC3000 has 52.9% similarity in a 420-aa overlap with YbtS, but 64.3% similarity in a 462-aa overlap with PchA of *P. aeruginosa* PAO1, which converts chorismate to isochorismate. PchA of *P. syringae* is similar to YbtS essentially in the chorismate binding domain, whereas the entire protein shows a similarity with PchA of *P. aeruginosa* (Fig. 5). Also, PchB of *P. syringae* DC3000 has 81.2% similarity in a 96-aa overlap with PchB of *P. aeruginosa* PAO1, which converts isochorismate to salicylate. The GC content of *pchA* and *pchB*, however, is different in *P. syringae* DC3000 (63.18% and only 58.26%, respectively) and in *P. aeruginosa* PAO1 (70.44% and 67.31%, respectively).

Gene organization in CFT073, the only *E. coli* strain whose YBT locus is sequenced (84), is the same as that in *Y. pestis*, but *irp1*, *irp2*, and *irp5*/*ybtE* would be modified into three open reading frames (ORFs) (c_2427, c_2428, and c_2429), two ORFs (c_2424 and c_2426), and two ORFs (c_2433 and c_2434), respectively. Depending on the annotated genome, the protein c_2433 is an ortholog of the enterobactin synthetase component E of *E. coli* K12 (NP_415126, b0594; 69.4% similarity in a 408-aa overlap), which activates 2,3-dihydroxybenzoate in catecholate siderophore synthesis (83). However, since c_2433 (415 aa) and c_2434 (94 aa) have 100% similarity with residues 1 to 413 and 432 to 525 of YbtE, respectively, it is clear that they are parts of a previous *irp5*/*ybtE* gene, which activates salicylate in phenolate siderophore synthesis (54, 83).

Comparisons between *P. syringae* pathovars. A YBT locus is present in *P. syringae* pv. tomato DC3000 (PSPTO2595, *pchA*, to PSPTO2606; Fig. 3B) and *P. syringae* pv. phaseolicola 1448A (PSPPH2904 to PSPPH2893) but absent in *P. syringae* pv. syringae B728a (8, 27, 36). The YBT locus gene organizations are totally identical in pathovars tomato and phaseolicola. The protein homologies range from 82.2% identity (93.5% similarity) for PchA to 95.1% identity (99.0% similarity) for PchB.

The YBT loci and the adjacent gene PSPTO2607 (Fig. 3B) or PSPPH2892 lie in a zone conserved in the three pathovars (Fig. 6): between homologues of the genes Psyr_2284 and Psyr_2285 of pathovar syringae. This intergenic region in pathovar syringae showed 88% identity in a 165-bp overlap with the side adjacent to PSPTO2608 in the 393-bp intergenic region between PSPTO2607 (Fig. 3B) and PSPTO2608 in pathovar tomato. In this common region, BLASTX indicated 49% similarity of a 59-aa sequence with a segment of the serine/threonine protein kinase MaK from *Arabidopsis thaliana* and 54% similarity of a 33-aa sequence with a segment of the NAD-dependent dehydrogenases COG0446 of *P. syringae* pv. syringae B728A. On the other hand, the 393-bp region between PSPTO2607 and PSPTO2608 showed 79% identity in, this time, a 371-bp overlap with the similar region in pathovar phaseolicola (between PSPPH2892 and PSPPH2891). The region common only to the pathovar phaseolicola contains a 70-bp AT-rich (84%) sequence that showed (BLASTN) 100% identity with 22-bp AT-rich sequences from *Homo sapiens* and *A. thaliana* and 90% identity with a 33-bp sequence from *H. sapiens*. The GC content is higher in the YBT locus than in the adjacent regions common in the three pathovars (Fig. 6).

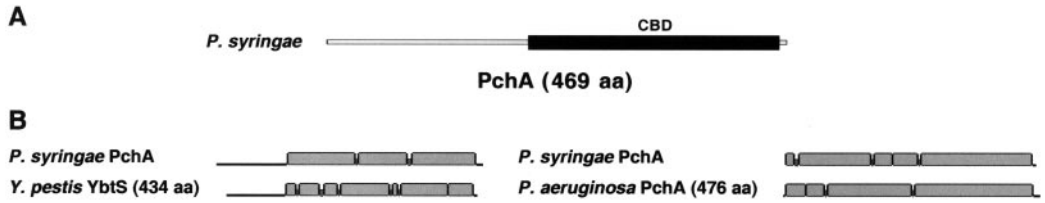

FIG. 5. (A) Location of the chorismate binding domain (CBD, black bar) detected in PchA of *P. syringae* DC3000 (gray bar) using the NCBI conserved domain search. (B) BLAST2 Sequences comparison of PchA of *P. syringae* DC3000 with either YbtS of *Y. pestis* 91001 or PchA of *P. aeruginosa* PAO1; the proteins are represented by thin lines, apart from zones with high similarity, which are represented by wide gray bars, and gaps, represented by intermediate-thickness dark gray bars.

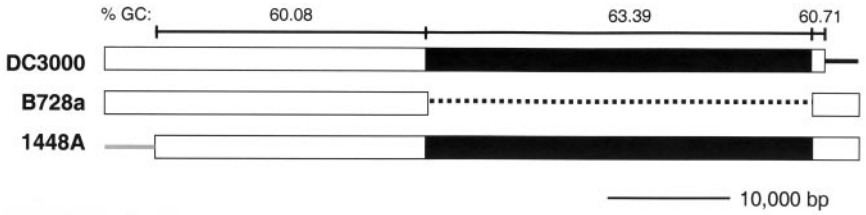

FIG. 6. Homologous regions around the YBT locus in *P. syringae* pv. tomato DC3000, *P. syringae* pv. syringae B728a, and *P. syringae* pv. phaseolicola 1448A and GC contents (*P. syringae* pv. tomato DC3000). Homologous regions are represented by rectangles; the YBT loci and the adjacent gene PSPTO2607 (DC3000) or PSPPH2892 (1448A) are black coded. Nonhomologous regions are shown either by a dark line when homologous proteins were found elsewhere in the genome of another strain or by a gray line when homologous proteins were not found anywhere in the genome of either of the other strains. The dotted line represents a gap. Homologous regions were determined by comparing protein or gene sequences using SSearch, BLASTP, or BLASTN and by comparing gene positions; protein homologies observed were higher than 80% identity. The last left and right genes represented that have a homologue in the same area in another pathovar are PSPTO2573 and PSPTO2609 (DC3000), Psyr_2264 and Psyr_2289 (B728a), and PSPPH2922 and PSPPH2887 (1448A); in 1448A, PSPPH2923 is an IS*801* transposase.

Search for mutations in *irp1 and irp2* in *E. coli* strains. Tests were conducted to establish whether the *E. coli* CFT073 modifications in the *irp2* and *irp1* homologues (Fig. 7A) were present and, consequently, the resulting proteins functional in the six YBT-producing ECOR strains. In *irp2*, the four PCR tests gave PCR products of about 189, 248, 132, and 192 bp, which indicated the absence of the IS*1541A*-like due 711-bp insertion in the ECOR strains and the correct expression of the *irp2* product HMWP2. In *irp1*, the sequenced segments were identical to the sequences of *Y. pestis* (Fig. 7B). We can conclude that there are differences in *irp1* and *irp2* between the strains investigated here and CFT073.

DISCUSSION

The study showed that YBT is produced by *P. syringae* and confirmed the highly probable involvement of the predicted YBT locus of *P. syringae* pv. tomato DC3000 (8) in YBT production. However, in this study, *irp1* was detected only in pathovars belonging to the genospecies 3, 7, and 8, as well as in the closely related pathovars phaseolicola and glycinea belonging to genospecies 2 (30, 49, 82). Although the presence of the YBT locus varies in a species (4, 14, 55, 58, 71), the separation observed within *P. syringae* was relatively clear. This may indicate the acquisition of the YBT locus by an ancestor of the producing pathovars and its stabilization in the chromosome or the acquisition of the YBT locus by an ancestor of *P. syringae* and a locus deletion in an ancestor of the nonproducing pathovars. This is confirmed by the identical locus organization and position in the genomes of the distant strains *P. syringae* pv. tomato DC3000 and *P. syringae* pv. phaseolicola 1448A, as well as by the protein heterogeneity in the YBT locus of these strains, which reflects a long evolution in *P. syringae*. A zone clearly involved in the insertion or the deletion of the YBT locus in *P. syringae* lies between PSPTO2607 and PSPTO2608 in pathovar tomato (between PSPPH2891 and PSPPH2892 in pathovar phaseolicola). The stability of the YBT locus in *P. syringae* was confirmed by the absence of integrase and IS elements in its proximity and by the observation that 92% of the strains from genospecies 3, 7, and 8 and pathovar morsprunorum race 2 possess the *irp1* gene. The PCR test could then be used in the diagnostic of the YBT-positive pathovars.

The YBT locus was functional in 10 pathovars out of 15. The HPLC-negative strains could produce less YBT or have nonfunctional or differently regulated genes. The advantage of producing YBT is unclear for strains producing both PVD and YBT; the very high stability constant of Fe-YBT (4×10^{36} compared with 10^{25} for the PVD) could carry an adaptive advantage in the competition for iron on the plant surface,

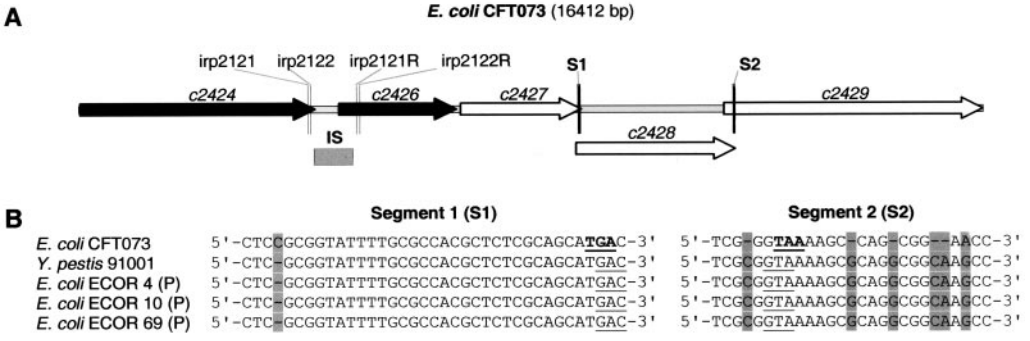

FIG. 7. (A) Map of the *irp2* and *irp1* homologous zones in *E. coli* CFT073, as annotated in its genome. Shown in the *irp2* zone are two ORFs (black arrows), a 711-bp IS*1541A*-like due insertion (IS), and the primers used in PCR analyses. Shown in the *irp1* zone are three ORFs (white arrows) and the modified segments S1 and S2. (B) Comparisons of S1 and S2 in *Y. pestis* and *E. coli*. In *E. coli* CFT073, modifications (gray) induce the lecture of stop codons (bold); in the next ORFs, the correct translation would restart downstream of the last base modification. No indication of this was found in the six YBT-producing ECOR strains, which indicates that *irp1* encodes HMWP1 in these strains.

even perhaps against other pseudomonads. However, the existence of genospecies 1, 2, 4, and 6 within which almost all of the strains are YBT negative probably indicates that pathogenicity is possible for *P. syringae* without producing YBT. This seems all the more probable because the PVD was not involved in the virulence of *P. syringae* pv. syringae (a YBT-negative pathovar) (Table 1) on cherry fruits (18), but this should be further confirmed by the study of negative mutants. The YBT locus could be a genomic island involved in the fitness and competitiveness of *P. syringae* rather than a pathogenicity island sensu stricto (14, 23, 69).

Two evolutionary lineages were described in HPI-positive enterobacteria (66, 70), but the differences observed between *Y. pestis*, *P. syringae*, and *P. luminescens* are of a greater magnitude. It is clear that three YBT locus evolutionary groups exist, of which two have been shown to be functional; all the HPI-positive enterobacteria belong to the *Y. pestis* group. The *P. syringae* and *P. luminescens* YBT locus organizations are quite similar, and both lack integrase. Since it is unlikely that excision from the HPI occurred in the same way in two species, it is possible that this gene organization resembles that of the YBT locus before its insertion in the HPI, but the understanding of the HPI formation is still conjectural (73). However, it is not clear whether the final product of the *P. luminescens* YBT locus is YBT, because the final polyketide synthase/peptide synthetase Plu2321 shows little similarity with, and is 745 aa longer than, HMWP1 of *Y. pestis*. Consequently, a YBT-related compound could be the final product in *P. luminescens*, as observed with a pseudomonad producing micacocidin, which resembles YBT (43). The *P. syringae* YBT locus would then represent an evolutionary link between the two systems.

In *P. syringae*, the presence of the isochorismate pyruvate lyase gene *pchB* and the deduced sequence of PchA strongly suggest that chorismate is converted to salicylate in a two-step mechanism. On the other hand, the YbtS homologue of *Y. enterocolitica* (Irp9) converts chorismate directly to salicylate; a similar function is supposed for MbtI in mycobactin synthesis (62, 65). PchA of *P. aeruginosa* is unable to effect the direct conversion (29). Since PchA of *P. syringae* is more similar to PchA of *P. aeruginosa* than to YbtS, it is probably also unable to effect this conversion. The presence of *pchB* in the YBT locus of *P. syringae* could indicate that a *pchB* homologue was present in the ancestor of the YBT locus, but the low GC content of *pchB* suggests that it could have an external origin. Also, since PchA showed the lowest similarity with its homologue in the *Y. pestis* or *P. luminescens* YBT locus (Table 3), it is not clear whether these proteins, which probably have slightly different functions, have a common ancestor in the YBT locus.

Nonpathogenic *E. coli* strains were investigated to develop the general *irp1*-based PCR test and to confirm the adaptability of the HPLC method. The ECOR collection represents the diversity of *E. coli* (57), but variations were observed between the same strains from three origins. This should be noted by those studying the ECOR strains.

The YBT-producing nonpathogenic ECOR strains tested in this study lack the modification in *irp1* and *irp2* found in the sequences of CFT073, which belongs to the uropathogenic group, responsible for acute cystitis and pyelonephritis. The production of YBT by CFT073 is not clear, because *irp5*/*ybtE*, encoding the salicyl-AMP ligase, is also disrupted, and the resulting protein, c_2433, is 110 aa shorter than Irp5. The high occurrence of the HPI in pathogenic *E. coli* suggests that it could be a virulence factor (5, 6, 16, 22, 37, 38, 39, 41, 44, 59, 70, 71, 72), although this is still a matter of debate (46). But HMWP1, HMWP2, or YBT was not detected in parts of populations recorded as positive for *irp1* and *irp2* using DNA hybridization and/or PCR (70, 71, 72). The CFT073 modifications in *irp1* are not detectable by the genetic methods used, and such modifications could be responsible for the observed results, since the inactivation of *irp1* down-regulated HMWP2, FyuA, and YBT synthesis in *Y. enterocolitica* (61). All the HPI-positive ECOR strains were positive when using HPLC in this study, and HPLC combined with the genetic procedures described could be used to explore the ability of human-pathogenic strains to produce YBT.

YBT detection methods are based on the detection or expression of genes and proteins of the YBT locus or on cross-feeding tests (55, 70, 71), but no method allows the molecule to be visualized. And yet this does provide the most unambiguous information. It is the second time that the solid-liquid technique in petri dishes (10) has proved to be an efficient way of producing siderophores, and it probably has potential for other genera and metabolites. The HPLC method for detecting YBT in the culture medium is similar to that described for PVDs (12) and comparable to the HPLC methods used to detect salicylic acid-based siderophores in concentrated supernatant extracts (2, 26, 51, 52, 68, 76). The method seems to be useful because YBT production appears to be more widely dispersed in the environment than previously thought and because it can be adapted for every environmental microorganism without having to grow potentially human-pathogenic indicator strains. It could be used to find new YBT producers, such as *P. luminescens*, perhaps, and new YBT locus groups irrespective of gene sequences. In addition, the *irp1* PCR test enables strains from two YBT locus groups to be simultaneously screened. The study of *E. coli* confirmed the usefulness of both methods.

ACKNOWLEDGMENTS

We thank J. R. Johnson, E. Denamur, and B. Picard for providing strains, J. R. Johnson for exchanging data, R. Rozenberg for the MS analyses, and Y. Muhovski for advice on the DNA hybridization study.

The work was supported by the Ministry of the Walloon Region (A.B. and I.G.) and by the Belgian National Fund for Scientific Research (E.D.H.).

REFERENCES

1. **Altschul, S. F., T. L. Madden, A. A. Schäffer, J. Zhang, Z. Zhang, W. Miller, and D. J. Lipman.** 1997. Gapped BLAST and PSI-BLAST: a new generation of protein database search programs. Nucleic Acids Res. **25:**3389–3402.
2. **Ankenbauer, R. G., T. Toyokuni, A. Staley, K. L. Rinehart, and C. D. Cox.** 1988. Synthesis and biological activity of pyochelin, a siderophore of *Pseudomonas aeruginosa*. J. Bacteriol. **170:**5344–5351.
3. **Ausubel, F. M., R. Brent, R. E. Kingston, D. D. Moore, J. G. Seidlan, J. A. Smith, and K. Struhl.** 2000. Current protocols in molecular biology. John Wiley & Sons, Inc., New York, N.Y.
4. **Bach, S., A. de Almeida, and E. Carniel.** 2000. The *Yersinia* high-pathogenicity island is present in different members of the family *Enterobacteriaceae*. FEMS Microbiol. Lett. **183:**289–294.
5. **Bingen-Bidois, M., O. Clermont, S. Bonacorsi, M. Terki, N. Brahimi, C. Loukil, D. Barraud, and E. Bingen.** 2002. Phylogenetic analysis and prevalence of urosepsis strains of *Escherichia coli* bearing pathogenicity island-like domains. Infect. Immun. **70:**3216–3226.
6. **Bonacorsi, S., O. Clermont, V. Houdouin, C. Cordevant, N. Brahimi, A.**

Marecat, C. Tinsley, X. Nassif, M. Lange, and E. Bingen. 2003. Molecular analysis and experimental virulence of French and North American *Escherichia coli* neonatal meningitis isolates: identification of a new virulent clone. J. Infect. Dis. **187:**1895–1906.

7. **Budzikiewicz, H.** 2004. Siderophores of the Pseudomonadaceae *sensu stricto* (fluorescent and non fluorescent *Pseudomonas* spp.), p. 81–237. *In* W. Herz, H. Falk, and G. W. Kirby (ed.), Progress in the chemistry of organic natural products, vol. 87. Springer, Vienna, Austria.
8. **Buell, C. R., V. Joardar, M. Lindeberg, J. Selengut, I. T. Paulsen, M. L. Gwinn, R. J. Dodson, R. T. Deboy, A. Scott Durkin, J. F. Kolonay, R. Madupu, S. Daugherty, L. Brinkac, M. J. Beanan, D. H. Haft, W. C. Nelson, T. Davidsen, N. Zafar, L. Zhou, J. Liu, Q. Yuan, H. Khouri, N. Fedorova, B. Tran, D. Russell, K. Berry, T. Utterback, S. E. Van Aken, T. V. Feldblyum, M. D'Ascenzo, W.-L. Deng, A. R. Ramos, J. R. Alfano, S. Cartinhour, A. K. Chatterjee, T. P. Delaney, S. G. Lazarowitz, G. B. Martin, D. J. Schneider, X. Tang, C. L. Bender, O. White, C. M. Fraser, and A. Collmer.** 2003. The complete genome sequence of the *Arabidopsis* and tomato pathogen *Pseudomonas syringae pv. tomato* DC3000. Proc. Natl. Acad. Sci. USA **100:**10181–10186.
9. **Bultreys, A., and I. Gheysen.** 1999. Biological and molecular detection of toxic lipodepsipeptide-producing *Pseudomonas syringae* strains and PCR identification in plants. Appl. Environ. Microbiol. **65:**1904–1909.
10. **Bultreys, A., and I. Gheysen.** 2000. Production and comparison of peptide siderophores from strains of distantly related pathovars of *Pseudomonas syringae* and *Pseudomonas viridiflava* LMG 2352. Appl. Environ. Microbiol. **66:**325–331.
11. **Bultreys, A., I. Gheysen, H. Maraite, and E. de Hoffmann.** 2001. Characterization of fluorescent and nonfluorescent peptide siderophores produced by *Pseudomonas syringae* strains and their potential use in strain identification. Appl. Environ. Microbiol. **67:**1718–1727.
12. **Bultreys, A., I. Gheysen., B. Wathelet, H. Maraite, and E. de Hoffmann.** 2003. High-performance liquid chromatography analyses of pyoverdin siderophores differentiate among phytopathogenic fluorescent *Pseudomonas* species. Appl. Environ. Microbiol. **69:**1143–1153.
13. **Bultreys, A., I. Gheysen, B. Wathelet, M. Schäfer, and H. Budzikiewicz.** 2004. The pyoverdins of *Pseudomonas syringae* and *Pseudomonas cichorii*. Z. Naturforsch. Sect. C. **59:**613–618.
14. **Carniel, E.** 2001. The *Yersinia* high-pathogenicity island: an iron-uptake island. Microbes Infect. **3:**561–569.
15. **Chambers, C. E., D. D. McIntyre, M. Mouck, and P. A. Sokol.** 1996. Physical and structural characterization of yersiniophore, a siderophore produced by clinical isolates of *Yersinia enterocolitica*. BioMetals **9:**157–167.
16. **Clermont, O., S. Bonacorsi, and E. Bingen.** 2001. The *Yersinia* high-pathogenicity island is highly predominant in virulence-associated phylogenetic groups of *Escherichia coli*. FEMS Microbiol. Lett. **196:**153–157.
17. **Cody, Y. S., and D. C. Gross.** 1987. Characterization of pyoverdin$_{pss}$, the fluorescent siderophore produced by *Pseudomonas syringae* pv. syringae. Appl. Environ. Microbiol. **53:**928–934.
18. **Cody, Y. S., and D. C. Gross.** 1987. Outer membrane protein mediating iron uptake via pyoverdin$_{pss}$, the fluorescent siderophore produced by *Pseudomonas syringae* pv. *syringae*. J. Bacteriol. **169:**2207–2214.
19. **Cornelis, P., and S. Matthijs.** 2002. Diversity of siderophore-mediated iron uptake systems in fluorescent pseudomonads: not only pyoverdines. Environ. Microbiol. **4:**787–798.
20. **Crosa, J. H., and C. T. Walsh.** 2002. Genetics and assembly line enzymology of siderophore biosynthesis in bacteria. Microbiol. Mol. Biol. Rev. **66:**223–249.
21. **Deng, W., V. Burland, G. Plunkett III, A. Boutin, G. F. Mayhew, P. Liss, N. T. Perna, D. J. Rose, B. Mau, S. Zhou, D. C. Schwartz, J. D. Fetherston, L. E. Lindler, R. R. Brubaker, G. V. Plano, S. C. Straley, K. A. McDonough, M. L. Nilles, J. S. Matson, F. R. Blattner, and R. D. Perry.** 2002. Genome sequence of *Yersinia pestis* KIM. J. Bacteriol. **184:**4601–4611.
22. **Dobrindt, U., G. Blum-Oehler, G. Nagy, G. Schneider, A. Johann, G. Gottschalk, and J. Hacher.** 2002. Genetic structure and distribution of four pathogenicity islands (PAI I_{536} to PAI IV_{536}) of uropathogenic *Escherichia coli* strain 536. Infect. Immun. **70:**6365–6372.
23. **Dobrindt, U., B. Hochhut, U. Hentschel, and J. Hacker.** 2004. Genomic islands in pathogenic and environmental microorganisms. Nat. Rev. Microbiol. **2:**414–424.
24. **Drechsel, H., H. Stephan, H. Lotz, H. Haag, H. Zähner, K. Hantke, and G. Jung.** 1995. Structure elucidation of yersiniabactin, a siderophore from highly virulent *Yersinia* strains. Liebigs. Ann. **1995:**1727–1733.
25. **Duchaud, E., C. Rusniok, L. Frangeul, C. Buchrieser, A. Givaudan, S. Taourit, S. Bocs, C. Boursaux-Eude, M. Chandler, J.-F. Charles, E. Dassa, R. Derose, S. Derzelle, G. Freyssinet, S. Gaudriault, C. Médigue, A. Lanois, K. Powell, P. Siguier, R. Vincent, V. Wingate, M. Zouine, P. Glaser, N. Boemare, A. Danchin, and F. Kunst.** 2003. The genome sequence of the entomopathogenic bacterium *Photorhabdus luminescens*. Nat. Biotechnol. **21:**1307–1313.
26. **Duffy, B. K., and G. Défago.** 1999. Environmental factors modulating antibiotic and siderophore biosynthesis by *Pseudomonas fluorescens* biocontrol strains. Appl. Environ. Microbiol. **65:**2429–2438.
27. **Feil, H., W. S. Feil, P. Chain, F. Larimer, G. DiBartolo, A. Copeland, A. Lykidis, S. Trong, M. Nolan, E. Goltsman, J. Thiel, S. Malfatti, J. E. Loper, A. Lapidus, J. C. Detter, M. Land, P. M. Richardson, N. C. Kyrpides, N. Ivanova, and S. E. Lindow.** 2005. Comparison of the complete genome sequences of *Pseudomonas syringae* pv. *syringae* B728a and pv. *tomato* DC3000. Proc. Natl. Acad. Sci. USA **102:**11064–11069.
28. **Gaille, C., P. Kast, and D. Haas.** 2002. Salicylate biosynthesis in *Pseudomonas aeruginosa*. J. Biol. Chem. **277:**21768–21775.
29. **Gaille, C., C. Reimmann, and D. Haas.** 2003. Isochorismate synthase (PchA), the first and rate-limiting enzyme in salicylate biosynthesis of *Pseudomonas aeruginosa*. J. Biol. Chem. **278:**16893–16898.
30. **Gardan, L., H. Shafik, S. Belouin, R. Broch, F. Grimont, and P. A. D. Grimont.** 1999. DNA relatedness among the pathovars of *Pseudomonas syringae* and description of *Pseudomonas tremae* sp. nov. and *Pseudomonas cannabina* sp. nov. (ex Sutic and Dowson 1959). Int. J. Syst. Bacteriol. **49:**469–478.
31. **Gehring, A. M., E. DeMoll, J. D. Fetherson, I. Mori, G. F. Mayhew, F. R. Blattner, C. T. Walsh, and R. D. Perry.** 1998. Iron acquisition in plague: modular logic enzymatic biogenesis of yersiniabactin by *Yersinia pestis*. Chem. Biol. **5:**573–586.
32. **Geoffroy, V. A., J. D. Fetherston, and R. D. Perry.** 2000. *Yersinia pestis* YbtU and YbtT are involved in synthesis of the siderophore yersiniabactin but have different effects on regulation. Infect. Immun. **68:**4452–4461.
33. **Haag, H., K. Hankte, H. Drechsel, I. Stojiljkovic, G. Jung, and H. Zähner.** 1993. Purification of yersiniabactin: a siderophore and possible virulence factor of *Yersinia enterocolitica*. J. Gen. Microbiol. **139:**2159–2165.
34. **Hartwig, R. C., and R. H. Loeppert.** 1993. Evaluation of soil iron, p. 465–482. *In* L. L. Barton and B. C. Hemming (ed.), Iron chelation in plants and soil microorganisms. Academic Press, San Diego, Calif.
35. **Hirano, S. S., and C. D. Upper.** 2000. Bacteria in the leaf ecosystem with emphasis on *Pseudomonas syringae*--a pathogen, ice nucleus, and epiphyte. Microbiol. Mol. Biol. Rev. **64:**624–653.
36. **Joardar, V., M. Lindeberg, R. W. Jackson, J. Selengut, R. Dodson, L. M. Brinkac, S. C. Daugherty, R. DeBoy, A. S. Durkin, M. G. Giglio, R. Madupu, W. C. Nelson, M. J. Rosovitz, S. Sullivan, J. Crabtree, T. Creasy, T. Davidsen, D. H. Haft, N. Zafar, L. Zhou, R. Halpin, T. Holley, H. Khouri, T. Feldblyum, O. White, C. M. Fraser, A. K. Chatterjee, S. Cartinhour, D. J. Schneider, J. Mansfield, A. Collmer, and C. R. Buell.** 2005. Whole-genome sequence analysis of *Pseudomonas syringae* pv. phaseolicola 1448A reveals divergence among pathovars in genes involved in virulence and transposition. J. Bacteriol. **187:**6488–6498.
37. **Johnson, J. R., and A. L. Stell.** 2000. Extended virulence genotypes of *Escherichia coli* strains from patients with urosepsis in relation to phylogeny and host compromise. J. Infect. Dis. **181:**261–272.
38. **Johnson, J. R., P. Delavari, M. Kuskowski, and A. L. Stall.** 2001. Phylogenetic distribution of extraintestinal virulence-associated traits in *Escherichia coli*. J. Infect. Dis. **183:**78–88.
39. **Johnson, J. R., T. T. O'Bryan, M. Kuskowski, and J. N. Maslow.** 2001. Ongoing horizontal and vertical transmission of virulence genes and *papA* alleles among *Escherichia coli* blood isolates from patients with diverse-source bacteremia. Infect. Immun. **69:**5363–5374.
40. **Jülich, M., K. Taraz, H. Budzikiewicz, V. Geoffroy, J.-M. Meyer, and L. Gardan.** 2001. The structure of the pyoverdin isolated from various *Pseudomonas syringae* pathovars. Z. Naturforsch. Sect. C. **56:**687–694.
41. **Karch, H., S. Schubert, D. Zhang, W. Zhang, H. Schmidt, T. Ölschläger, and J. Hacker.** 1999. A genomic island, termed high-pathogenicity island, is present in certain non-O157 shiga toxin-producing *Escherichia coli* clonal lineages. Infect. Immun. **67:**5994–6001.
42. **King, E. O., M. K. Ward, and D. E. Raney.** 1954. Two simple media for the demonstration of pyocyanin and fluorescein. J. Lab. Clin. Med. **44:**301–307.
43. **Kobayashi, S., H. Nakai, Y. Ikenishi, W. Y. Sun, M. Ozaki, Y. Hayase, and R. Takeda.** 1998. Micacocidin A, B and C, novel antimycoplasma agents from *Pseudomonas* sp. II. Structure elucidation. J. Antibiot. **51:**328–332.
44. **Koczura, R., and A. Kaznowski.** 2003. The *Yersinia* high-pathogenicity island and iron-uptake systems in clinical isolates of *Escherichia coli*. J. Med. Microbiol. **52:**637–642.
45. **Kunkle, C. A., and M. P. Schmitt.** 2003. Analysis of the *Corynebacterium diphtheriae* DtxR regulon: identification of a putative siderophore synthesis and transport system that is similar to the *Yersinia* high-pathogenicity island-encoded yersiniabactin synthesis and uptake system. J. Bacteriol. **185:**6826–6840.
46. **Lefranc Nègre, V., S. Bonacorsi, S. Schubert, P. Bidet, X. Nassif, and E. Bingen.** 2004. The siderophore receptor iroN, but not the high-pathogenicity island or the hemin receptor chuA, contributes to the bacteremic step of *Escherichia coli* neonatal meningitis. Infect. Immun. **72:**1216–1220.
47. **Loper, J. E., and S. E. Lindow.** 1987. Lack of evidence for in situ fluorescent pigment production by *Pseudomonas syringae pv. syringae* on bean leaf surfaces. Phytopathology **77:**1449–1454.
48. **Loper, J. E., and. M. D. Henkels.** 1997. Availability of iron to *Pseudomonas fluorescens* in rhizosphere and bulk soil evaluated with an ice nucleation reporter gene. Appl. Environ. Microbiol. **63:**99–105.

49. **Marques, A. S. D. A., R. Corbière, L. Gardan, C. Tourte, C. Manceau, J. D. Taylor, and R. Samson.** 2000. Multiphasic approach for the identification of the different classification levels of *Pseudomonas savastanoi* pv. phaseolicola. Eur. J. Plant Pathol. **106:**715–734.
50. **Martins dos Santos, V. A. P., S. Heim, E. R. B. Moore, M. Strätz, and K. N. Timmis.** 2004. Insights into the genomic basis of niche specificity of *Pseudomonas putida* KT2440. Environ. Microbiol. **6:**1264–1286.
51. **Maurhofer, M., C. Reimmann, P. Schmidli-Sacherer, S. Heeb, D. Haas, and G. Défago.** 1998. Salicylic acid biosynthetic genes expressed in *Pseudomonas fluorescens* strain P3 improve the induction of systemic resistance in tobacco against tobacco necrosis virus. Phytopathology **88:**678–684.
52. **Mercado-Blanco, J., K. M. G. M. van der Drift, P. E. Olsson, J. E. Thomas-Oates, L. C. van Loon, and P. A. H. M. Bakker.** 2001. Analysis of the *pmsCEAB* gene cluster involved in biosynthesis of salicylic acid and the siderophore pseudomonine in the biocontrol strain *Pseudomonas fluorescens* WCS374. J. Bacteriol. **183:**1909–1920.
53. **Meyer, J.-M., V. A. Geoffroy, N. Baida, L. Gardan, D. Izard, P. Lemanceau, W. Achouak, and N. J. Palleroni.** 2002. Siderophore typing, a powerful tool for the identification of fluorescent and nonfluorescent pseudomonads. Appl. Environ. Microbiol. **68:**2745–2753.
54. **Miller, D. A., L. Luo, N. Hillson, T. A. Keating, and C. T. Walsh.** 2002. Yersiniabactin synthetase: a four-protein assembly line producing the nonribosomal peptide/polyketide hybrid siderophore of *Yersinia pestis*. Chem. Biol. **9:**333–334.
55. **Mokracka, J., R. Koczura, and A. Kaznowski.** 2004. Yersiniabactin and other siderophores produced by clinical isolates of *Enterobacter* spp. and *Citrobacter* spp. FEMS Immunol. Med. Microbiol. **40:**51–55.
56. **Myers, E. W., and W. Miller.** 1988. Optimal alignments in linear space. Comput. Appl. Biosci. **4:**11–17.
57. **Ochman, H., and R. K. Selander.** 1984. Standard reference strains of *Escherichia coli* from natural populations. J. Bacteriol. **157:**690–693.
58. **Oelschlaeger, T. A., D. Zhang, S. Schubert, E. Carniel, W. Rabsch, H. Karch, and J. Hacker.** 2003. The high-pathogenicity island is absent in human pathogens of *Salmonella enterica* subspecies I but present in isolates of subspecies III and VI. J. Bacteriol. **185:**1107–1111.
59. **Okeke, I. N., I. C. A. Scaletsky, E. H. Soars, L. R. Macfarlane, and A. G. Torres.** 2004. Molecular epidemiology of the iron utilization genes of enteroaggregative *Escherichia coli*. J. Clin. Microbiol. **42:**36–44.
60. **Parkhill, J., B. W. Wren, N. R. Thomson, R. W. Titball, M. T. G. Holden, M. B. Prentice, M. Sebaihia, K. D. James, C. Churcher, K. L. Mungall, S. Baker, D. Basham, S. D. Bentley, K. Brooks, A. M. Cerdeno-Tárraga, T. Chillingworth, A. Cronin, R. M. Davies, P. Davis, G. Dougan, T. Feltwell, N. Hamlin, S. Holroyd, K. Jagels, A. V. Karlyshev, S. Leather, S. Moule, P. C. F. Oyston, M. Quail, K. Rutherford, M. Simmonds, J. Skelton, K. Stevens, S. Whitehead, and B. G. Barrell.** 2001. Genome sequence of *Yersinia pestis*, the causative agent of plague. Nature **413:**523–527.
61. **Pelludat, C., A. Rakin, C. A. Jacobi, S. Schubert, and J. Heesemann.** 1998. The yersiniabactin biosynthetic gene cluster of *Yersinia enterocolitica*: organization and siderophore-dependent regulation. J. Bacteriol. **180:**538–546.
62. **Pelludat, C., D. Brem, and J. Heesemann.** 2003. Irp9, encoded by the high-pathogenicity island of *Yersinia enterocolitica*, is able to convert chorismate into salicylate, the precursor of the siderophore yersiniabactin. J. Bacteriol. **185:**5648–5653.
63. **Perry, R. D., P. B. Balbo, H. A. Jones, J. D. Fetherston, and E. DeMoll.** 1999. Yersiniabactin from *Yersinia pestis*: biochemical characterization of the siderophore and its role in iron transport and regulation. Microbiology **145:** 1181–1190.
64. **Perry, R. D.** 2004. *Yersinia*, p. 219–240. *In* J. H. Crosa, A. R. Mey, and S. M. Payne (ed.), Iron transport in bacteria. American Society for Microbiology, Washington, D.C.
65. **Quadri, L. E. N., J. Sello, T. A. Keatin, P. H. Weinreb, and C. T. Walsh.** 1998. Identification of a *Mycobacterium tuberculosis* gene cluster encoding the biosynthetic enzymes for assembly of the virulence-conferring siderophore mycobactin. Chem. Biol. **5:**631–645.
66. **Rakin, A., P. Urbitsch, and J. Heesemann.** 1995. Evidence for two evolutionary lineages of highly pathogenic *Yersinia* species. J. Bacteriol. **177:**2292–2298.
67. **Ratledge, C., and L. G. Dover.** 2000. Iron metabolism in pathogenic bacteria. Annu. Rev. Microbiol. **54:**881–941.
68. **Reimmann, C., H. M. Patel, C. T. Walsh, and D. Haas.** 2004. PchC thioesterase optimizes nonribosomal biosynthesis of the peptide siderophore pyochelin in *Pseudomonas aeruginosa* J. Bacteriol. **186:**6367–6373.
69. **Schmidt, H., and M. Hensel.** 2004. Pathogenicity islands in bacterial pathogenesis. Clin. Microbiol. Rev. **17:**14–56.
70. **Schubert, S., A. Rakin, H. Karch, E. Carniel, and J. Heeseman.** 1998. Prevalence of the "high-pathogenicity island" of *yersinia* species among *Escherichia coli* strains that are pathogenic to humans. Infect. Immun. **66:**480–485.
71. **Schubert, S., S. Cuenca, D. Fischer, and J. Heesemann.** 2000. High-pathogenicity island of *Yersinia pestis* in enterobacteriaceae isolated from blood cultures and urine samples: prevalence and functional expression. J. Infect. Dis. **182:**1268–1271.
72. **Schubert, S., B. Picard, S. Gouriou, J. Heesemann, and E. Denamur.** 2002. *Yersinia* high-pathogenicity island contributes to virulence in *Escherichia coli* causing extraintestinal infections. Infect. Immun. **70:**5335–5337.
73. **Schubert, S., S. Dufke, J. Sorsa, and J. Heeseman.** 2004. A novel integrative and conjugative element (ICE) of *Escherichia coli*: the putative progenitor of the *Yersinia* high-pathogenicity island. Mol. Microbiol. **51:**837–848.
74. **Schwyn, B., and J. B. Neilands.** 1986. Universal chemical assay for the detection and determination of siderophores. Anal. Biochem. **160:**47–56.
75. **Serino, L., C. Reimmann, H. Baur, M. Beyeler, P. Visca, and D. Haas.** 1995. Structural genes for salicylate biosynthesis from chorismate in *Pseudomonas aeruginosa*. Mol. Gen. Genet. **249:**217–228.
76. **Serino, L., C. Reimmann, P. Visca, M. Beyeler, V. D. Chiesa, and D. Haas.** 1997. Biosynthesis of pyochelin and dihydroaeruginoic acid requires the iron-regulated *pchDCBA* operon in *Pseudomonas aeruginosa*. J. Bacteriol. **179:**248–257.
77. **Simon, E. H., and I. Tessman.** 1963. Thymidine-requiring mutants of phage T4. Proc. Natl. Acad. Sci. USA **50:**526–532.
78. **Smith, T. F., and M. S. Waterman.** 1981. Identification of common molecular subsequences. J. Mol. Biol. **147:**195–197.
79. **Smith, E. E., E. H. Sims, D. H. Spencer, R. Kaul, and M. V. Olson.** 2005. Evidence for diversifying selection at the pyoverdine locus of *Pseudomonas aeruginosa*. J. Bacteriol. **187:**2138–2147.
80. **Song, Y., Z. Tong, J. Wang, L. Wang, Z. Guo, Y. Han, J. Zhang, D. Pei, D. Zhou, H. Qin, X. Pang, Y. Han, J. Zhai, M. Li, B. Cui, Z. Qi, L. Jin, R. Dai, F. Chen, S. Li, C. Ye, Z. Du, W. Lin, J. Wang, J. Yu, H. Yang, J. Wang, P. Huang, and R. Yang.** 2004. Complete genome sequence of *Yersinia pestis* strain 91001, an isolate avirulent to humans. DNA Res. **11:**179–197.
81. **Tatusova, T. A., and T. L. Madden.** 1999. BLAST 2 Sequences, a new tool for comparing protein and nucleotide sequences. FEMS Microbiol. Lett. **174:** 247–250.
82. **Völksch, B., and H. Weingart.** 1997. Comparison of ethylene-producing *Pseudomonas syringae* strains isolated from kudzu (*Pueraria lobata*) with *Pseudomonas syringae* pv. phaseolicola and *Pseudomonas syringae* pv. glycinea. Eur. J. Plant Pathol. **103:**795–802.
83. **Walsh, C. T., and C. G. Marshall.** 2004. Siderophore biosynthesis in bacteria, p. 18–37. *In* J. H. Crosa, A. R. Mey, and S. M. Payne (ed.), Iron transport in bacteria. American Society for Microbiology, Washington, D.C.
84. **Welch, R. A., V. Burland, G. Plunkett, P. Redford, P. Roesch, D. Rasko, E. L. Buckles, S.-R. Liou, A. Boutin, J. Hackett, D. Stroud, G. F. Mayhew, D. J. Rose, S. Zhou, D. C. Schwartz, N. T. Perna, H. L. T. Mobley, M. S. Donnenberg, and F. R. Blattner.** 2002. Extensive mosaic structure revealed by the complete genome sequence of uropathogenic *Escherichia coli*. Proc. Natl. Acad. Sci. USA **99:**17020–17024.